Multi-wavelength, all-solid-state, continuous wave mode locked picosecond Raman laser

Eduardo Granados,[1,*] Helen M. Pask,[1] Elric Esposito,[2] Gail McConnell,[2] and David J. Spence[1]

[1] *MQ Photonics Research Centre, Department of Physics and Engineering, Macquarie University, 2109 New South Wales, Australia*

[2] *Centre for Biophotonics, Strathclyde Institute for Pharmacy and Biomedical Sciences, University Of Strathclyde, 27 Taylor St, Glasgow G4 0NR, United Kingdom*

[*] *granados@ics.mq.edu.au*

Abstract: We demonstrate the operation of a cascaded continuous wave (CW) mode-locked Raman oscillator. The output pulses were compressed from 28 ps at 532 nm down to 6.5 ps at 559 nm (first Stokes) and 5.5 ps at 589 nm (second Stokes). The maximum output was 2.5 W at 559 nm and 1.4 W at 589 nm with slope efficiencies up to 52%. This technique allows simple and efficient generation of short-pulse radiation to the cascaded Stokes wavelengths, extending the mode-locked operation of Raman lasers to a wider range of visible wavelengths between 550 – 700 nm based on standard inexpensive picosecond neodymium-based oscillators.

OCIS codes: (140.3550) Lasers, Raman; (320.5520) Pulse compression; (180.0180) Microscopy

References and links

1. J. M. Girkin, and G. McConnell, "Advances in laser sources for confocal and multiphoton microscopy," Microsc. Res. Tech. **67**, 8-14 (2005).
2. G. McConnell, G. L. Smith, J. M. Girkin, A. M. Gurney, and A. I. Ferguson, "Two-photon microscopy of fura-2-loaded cardiac myocytes with an all-solid-state tunable and visible femtosecond laser source," Opt. Lett. **28**, 1742-1744 (2003).
3. J. Palero, V. Boer, J. Vijverberg, H. Gerritsen, and H. J. C. M. Sterenborg, "Short-wavelength two-photon excitation fluorescence microscopy of tryptophan with a photonic crystal fiber based light source," Opt. Express **13**, 5363-5368 (2005).
4. H. M. Pask, P. Dekker, R. P. Mildren, D. J. Spence, and J. A. Piper, "Wavelength-versatile visible and UV sources based on crystalline Raman lasers," Prog. Quantum Electron. **32**, 121-158 (2008).
5. R. Mildren, M. Convery, H. Pask, J. Piper, and T. McKay, "Efficient, all-solid-state, Raman laser in the yellow, orange and red," Opt. Express **12**, 785-790 (2004).
6. E. Granados, H. M. Pask, and D. J. Spence, "Synchronously pumped continuous-wave mode-locked yellow Raman laser at 559 nm," Opt. Express **17**, 569-574 (2009).
7. G. G. Grigoryan and S. B. Sogomonyan, "Synchronously pumped picosecond Raman laser utilizing an $LiIO_3$ crystal," Sov. J. Quantum Electron., 1402 (1989).
8. E. Granados, A. Fuerbach, D. Coutts, and D. Spence, "Asynchronous cross-correlation for weak ultrafast deep ultraviolet laser pulses," Appl. Phys. B (to be published).
9. A. Penzkofer, A. Laubereau, and W. Kaiser, "High intensity Raman interactions," Prog. Quantum Electron. **6**, 55-140 (1979).
10. T. Basiev, P. Zverev, A. Karasik, V. Osiko, A. Sobol', and D. Chunaev, "Picosecond stimulated Raman scattering in crystals," J. Exp. Theor. Phys. **99**, 934-941 (2004).
11. L. Lefort, K. Puech, S. D. Butterworth, Y. P. Svirko, and D. C. Hanna, "Generation of femtosecond pulses from order-of-magnitude pulse compression in a synchronously pumped optical parametric oscillator based on periodically poled lithium niobate," Opt. Lett. **24**, 28-30 (1999).

1. Introduction

There is considerable interest in the development of picosecond pulse laser sources in the visible region between 500 and 650 nm. Applications such as two-photon microscopy can use this radiation for matching the two-photon absorption bands of a wide range of biological samples, either capitalising upon endogenous autofluorescent structures or synthetic fluorophores that serve as the contrast mechanism. Given the nonlinear nature of the excitation, it is desirable to use a laser source generating picosecond or femtosecond pulses; such sources have high peak power to enhance the non-linear two photon process while maintaining a low average power to avoid damage to the biological sample under investigation. Perfect wavelength matching to the absorption bands of the fluorophores of interest is not usually required, since they tend to be fairly broad (20 – 30 nm) [1].

Several approaches have been explored to generate suitable laser pulses for this application. For example, optical parametric oscillators have been used to generate tunable ultrafast radiation from the UV to the IR [2], but such systems are typically expensive and complex. Photonic crystal fibers have been also employed to produce tunable pulses of several picoseconds in the 500 – 600 nm range [3], but the average power associated with this source was low, allowing only near-threshold two-photon absorption. A third possibility is to employ a femtosecond-pulsed Ti:Sapphire or Nd-based laser for three-photon absorption. However, the peak power requirements for three-photon absorption significantly exceed that for two-photon microscopy and hence this technique has limited applications in biological imaging. There is therefore keen interest and motivation to explore different alternatives that can offer increased simplicity and lower cost for two-photon microscopy.

Raman shifting of conventional lasers to access new wavelengths is a well established technique [4]. In particular, stimulated Raman scattering (SRS) in crystalline media has been widely used in a variety of configurations to efficiently generate IR, visible and UV output [4, 5]. Using a cavity around a Raman medium allows effective control over the conversion and cascading of the SRS process to second and higher Stokes orders, allowing the desired Stokes order to be selectively output and even allowing several wavelengths to be output simultaneously. Synchronously pumped Raman lasers have been demonstrated as an efficient route for the generation of picosecond pulses at certain visible and IR wavelengths [6, 7].

In this Letter, we report a synchronously pumped mode locked Raman laser generating two different wavelengths using cascaded Raman shifting in a multi-cavity arrangement. We produced 2.4 W at 559 nm and 1.4 W at 589 nm, with slope efficiencies up to 52% for both Stokes wavelengths. The peak power of the generated pulses was almost as high as the pump pulses as a consequence of pulse shortening.

2. Experiments

A 50 × 5 × 5 mm potassium gadolinium tungstate (KGW) crystal (anti reflection coated at 532 nm, normal incidence) was used in the experiments as the SRS gain medium. This crystal was pumped along its N_m axis to match the 901 cm^{-1} Raman shift, corresponding to a first Stokes wavelength of 559 nm and a second Stokes wavelength of 589 nm. The resonator design is depicted in Fig 1, and was essentially a z-fold design. Concave mirrors (M_1, M_2), each with a 20 cm radius of curvature, were separated by approximately 23 cm. This mirror separation led to a mode waist radius of 33 μm centred in the KGW crystal. The angle of the z-fold cavity was kept small to minimize the astigmatism of the cavity mode. For effective control over the cascading process, we arranged a pair of high dispersion F5 prisms (P_1 and P_2) to spatially separate the Stokes wavelengths onto different end mirrors, thereby forming separate cavities with independent control of both cavity length and output coupling for each Stokes mode. The first Stokes mode impinged on M_4, while the second Stokes mode, when present, was directed to M_5 by a small scraper mirror. The mirrors M_1, M_2 and M_3 were high reflectors for the Stokes wavelengths. Although the laser was designed for the Stokes radiation to be output through mirrors M_4 and M_5 only, there was also some leakage at 559 and 589 nm through the other cavity mirrors. Accordingly, the reported output powers are the

sum from the output coupler and the small leakages through the other imperfect mirrors. Mirrors M_4 and M_5 were translated to achieve the correct cavity length to ensure that the circulation of the intracavity fields was synchronized with the inter pulse period of the pump laser, as required for synchronous mode locking.

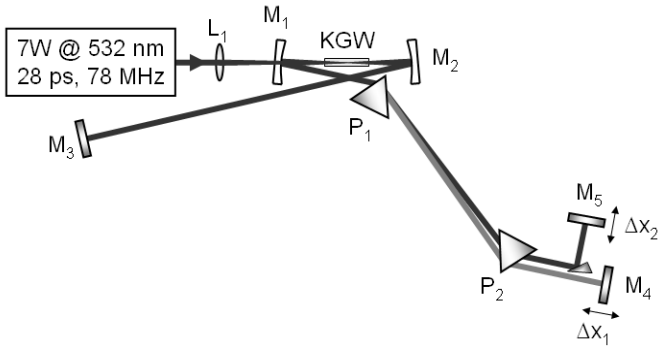

Fig. 1. Setup for the multi-cavity continuous-wave mode-locked Raman oscillator.

The pump laser was a CW mode-locked Nd:YAG laser producing 22 W at 1064 nm with a repetition rate of 78 MHz. The pump radiation was frequency doubled by non-critically phase-matched second harmonic generation in a 3.5 cm long lithium triborate (LBO) crystal. The generated output power at 532 nm was approximately 7 W with a pulse duration of 28 ps.

When optimized to output first Stokes only, mirror M_4 was an 80% transmission output coupler at 559 nm. There was no further cascading to the second Stokes wavelength. Figure 2 shows the slope efficiency for the first Stokes (open circles): The maximum CW output power was 2.5 W at 559 nm for an incident power of 6.5 W, reaching a maximum green to yellow optical conversion efficiency of 38.4%, and with a slope efficiency of 52%.

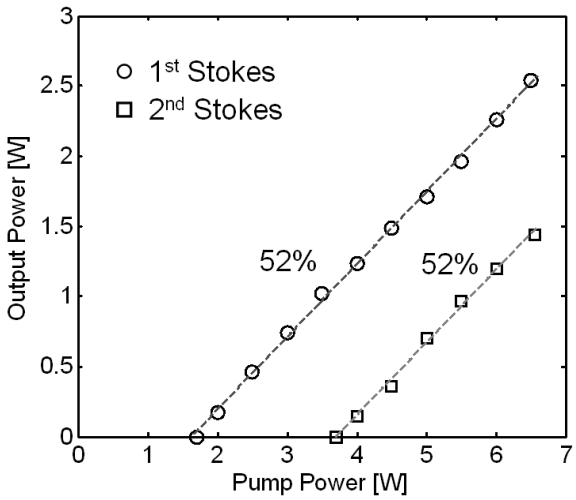

Fig. 2. Slope efficiencies for optimized resonators for 1st Stokes (open circles) and 2nd Stokes (open squares)

When optimized to cascade to the second Stokes wavelength, both fields were overlapped in the laser crystal but spatially separated onto mirrors M_4 and M_5; M_4 was a high reflector at 559 nm and M_5 was an 80% output coupler at 589 nm. Fine adjustment of each cavity length was necessary to effectively match the optimum cavity length at each Stokes wavelengths. Figure 2 shows the slope efficiency for the second Stokes (open squares): The maximum

output power at 589 nm was 1.4 W, which was an optical conversion efficiency of 21.5%. The slope efficiency in this case was also 52%.

We note that by adding a third cavity, aligned for third Stokes, we were able to generate more than 100 mW at 620 nm. In this the case the output coupler for the second Stokes was replaced with a high reflector; however substantial leakage of the second Stokes field through the other mirrors acted as a substantial loss for that field and so the laser was far from optimized for generating 620 nm. Higher output powers at 620 nm can be anticipated by optimization of the resonator mirror coatings.

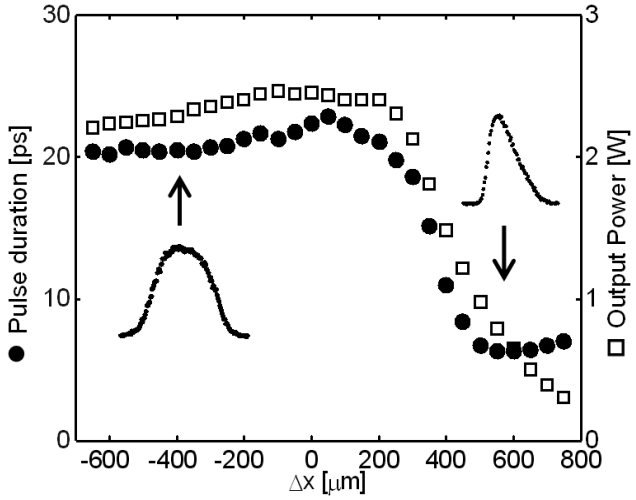

Fig. 3 Output pulse duration (filled circles) and Output power (open squares) changing the cavity length for the 1st Stokes. (inset) Cross correlations of the output yellow pulses for different cavity length detunings.

For the above results, the cavity lengths were optimized to achieve the highest output powers. However, for different cavity lengths, the laser displayed substantial pulse compression, due to the complex interplay between the non-instantaneous Raman effect and the depletion of the pump field. Accurate retrieval of the output pulse shapes has significant importance to correctly interpret the intracavity dynamics of the laser; to recover the pulse profiles we used an asynchronous cross-correlation technique [8]. Figure 3 shows the dependence of pulse duration and output power on the cavity length detuning for the first Stokes output (Δx_1). We define the cavity length detuning (Δx_1 and Δx_2) for each wavelength as the difference in the cavity length from that corresponding to the minimum threshold for laser operation for each wavelength. We observed that the pulse compression reached its maximum when the cavity detuning was approximately $\Delta x_1 = +500$ μm. The shortest pulses had a duration of 6.5 ps (compression factor >4). The temporal pulse shape is shown inset in Fig 3, and it can be seen that the pulse was asymmetric, with a steep leading edge. In regions of strong compression, the peak power was increased even though the output power was reduced: the highest peak power at 559 nm was 1.92 kW for a cavity length of $\Delta x_1 = +450$ μm. For cavity length detunings $\Delta x_1 < +200$ μm, the output power and pulse duration showed a long plateau that extended down to $\Delta x_1 = -2500$ μm (well beyond the range of the figure). In this region, the peak power was approximately 1.4 kW.

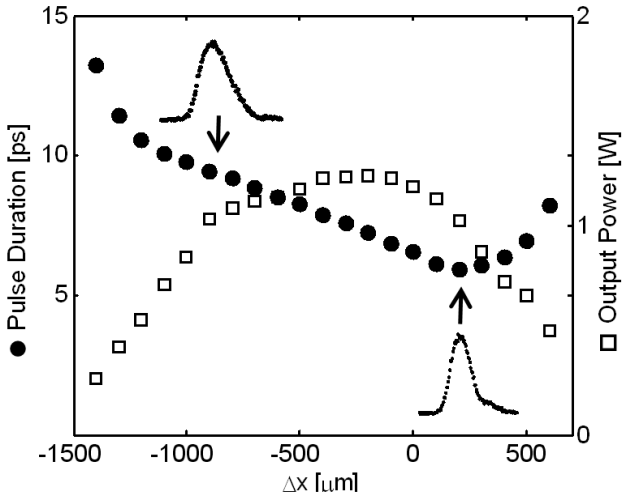

Fig. 4 Output pulse duration (filled circles) and Output power (open squares) changing the cavity length for the 2nd Stokes. (inset) Cross correlations of the output orange pulses for different cavity length detunings.

For the next measurements, the cavity lengths of the 1st Stokes and 2nd Stokes were first adjusted simultaneously to maximize the output power at 589 nm, found for first-Stokes cavity length of $\Delta x_1 = 280$ μm. Figure 4 then shows the output power and pulse duration as a function of 2nd Stokes cavity length Δx_2. We observed that the orange pulses where shortest when the cavity detuning was approximately $\Delta x_2 = +200$ μm. Those pulses had a duration of 5.5 ps (compression factor >5 from green to orange), and exhibited a small shoulder as shown in the inset cross-correlated traces of Figure 4. In contrast with the behavior of the compression of the 1st Stokes pulses, in this case, the output power was close to its maximum when the pulse compression occurred, suggesting that the compression mechanism for 2nd Stokes was different from the 1st Stokes. The maximum peak power of 2.95 kW was measured at $\Delta x_2 = +100$ μm, and the maximum output power was 1.4 W. Table 1 summarizes the results for 1st and 2nd Stokes in different arrangements.

Table 1. Summary of results

	λ	Max Peak Power	Min Pulse duration	Max Output Power
Pump	532 nm	3.2 kW	28 ps	6.5 W
1st Stokes	559 nm	1.92 kW ($\Delta x_1 = +450$ μm)	6.5 ps ($\Delta x_1 = +500$ μm)	2.5 W ($\Delta x_1 = -100$ μm)
2nd Stokes	589 nm	2.95 kW ($\Delta x_2 = +100$ μm)	5.5 ps ($\Delta x_2 = +200$ μm)	1.4 W ($\Delta x_2 = -200$ μm)

3. Discussion and conclusion

Separate optimization of the physical cavity lengths for the different wavelengths is vital for effective operation of this cascaded Raman laser. The group delay difference traversing the 50 mm KGW crystal between first Stokes and pump is 4.2 ps, with a similar delay between the second and first Stokes. This is normal dispersion with the longer wavelength travelling faster. The substantial difference between the first and second Stokes is the reason that separately adjustable cavities were required to optimize second Stokes generation. The successive compression of the generated pulses is caused in part by this group delay mismatch through the crystal, although in this case the mismatch was relatively small in comparison with the pump pulse duration, and so compression of the 1st Stokes pulse was not as effective as for shorter pump pulses [6]. The group delay differences (GDD) created by the prism pair

was approximately -1 ps between the first and second Stokes, and so partially compensates for the GDD of the KGW. In principle, with a much longer prism separation, the prism pair could be used to optimize the relative cavity lengths of the first and second Stokes. However using the prisms to separate the wavelengths onto different end mirrors allows much greater flexibility, both to tune the path lengths and to individually tailor the reflectivity of each mirror.

It is important to understand the effect of cavity length detuning on the behavior of the pulses in the cavity. Consider first the behavior of the pump and first stokes pulses. If the cavity detuning is zero, then the round trip time at the Stokes group velocity is exactly equal to the interpulse period of the pump laser. The group delay difference between the wavelengths means that the Stokes pulse overtakes the pump pulse by 2.2 ps during the pass through the crystal, but the cavity length is such that the relative positions of the pulses are the same after each round trip.

If the cavity is lengthened, it would at first appear that the Stokes pulse must arrive later and later compared to the pump pulse on each round trip. However, the relative positions of the pump and Stokes pulses after each round trip must actually still be the same since the laser is operating in steady-state. The lag is actually counteracted on each round trip by a reshaping of the Stokes pulse during the pass through crystal – in this case by preferential amplification of the leading edge of the Stokes pulse so that the amplified Stokes pulse is formed at a slightly advanced position. As the cavity detuning becomes more severe, a more severe pulse reshaping must take place requiring higher gain, and eventually the laser drops below threshold.

There is a strong asymmetry of the laser behavior with the sign of the cavity length detuning. This is due to fact that we are in the regime of transient Raman scattering; according to [9], transient effects have to be taken into account for pulse durations less than 20 times the dephasing time for the molecular transition. Our pump pulse duration is 28 ps and the dephasing time of KGW is 2.1 ps [10]), and so we must account for the accumulation of phonons during each pulse. This accumulation makes the Stokes gain far higher for the trailing edge of the Stokes pulse. Negative detuning corresponds to the Stokes pulse arriving at the crystal a little early on each round trip and therefore needing to be mostly amplified on the trailing edge - this is also favored transient scattering regime and means that much more negative detuning can be tolerated than positive detuning.

The pulse compression results from the Stokes pulse sweeping through the pump pulse during the crystal transit owing to the differing velocities, allowing a shorter Stokes pulse to sweep the energy out of a longer pump pulse [11]. Compression is most effective for positive detuning, corresponding to the Stokes pulse arriving at the crystal a little after the pump pulse. In this case, the reshaping of the pulse to advance its position reinforces the sweep of the Stokes pulse through the pump pulse, enhancing the compression effect. Since the leading edge of the Stokes pulse is advancing through undepleted regions of the pump pulse, we see steepening of the leading edge, as measured for positive detunings in Figure 3. To fully understand this compression and the effect of transient Raman scattering, numerical modeling is required.

In conclusion, we have demonstrated a cascaded continuous-wave mode-locked Raman laser producing 2.5 W at 559 nm and 1.4 W at 589 nm. Slope efficiencies up to 52% were obtained for both 1st and 2nd Stokes by independent optimization of the output coupling and cavity length for each Stokes order. By adding a third cavity to the setup, we were able to generate 3rd Stokes radiation, producing more than 100 mW at 620 nm. We anticipate the possibility of further cascading to red wavelengths using this technique; generating an infrared cascade using 1064 nm pump radiation is also clearly available. Overall green-yellow and green-orange efficiencies of up to 38.4% and 21.5% respectively were demonstrated, and the shortest pulses obtained correspond to 6.5 ps at 559 nm and 5.5 ps at 589 nm. These flexible and robust picosecond laser pulses should find many applications, particularly in biological imaging.